Developmental Cell
Article

The Hippo Pathway Regulates Wnt/β-Catenin Signaling

Xaralabos Varelas,[1,2] Bryan W. Miller,[3,5] Richelle Sopko,[2,4] Siyuan Song,[3,5] Alex Gregorieff,[1,2] Frederic A. Fellouse,[1,2] Rui Sakuma,[1,2] Tony Pawson,[1,2,4] Walter Hunziker,[6] Helen McNeill,[2,4] Jeffrey L. Wrana,[1,2,4] and Liliana Attisano[3,5,*]
[1]Center for Systems Biology
[2]Samuel Lunenfeld Research Institute
Mount Sinai Hospital, 600 University Avenue, Toronto, ON M5G 1X5, Canada
[3]Department of Biochemistry
[4]Department of Molecular Genetics
[5]Donnelly Centre for Cellular and Biomolecular Research
University of Toronto, 160 College Street, Toronto, ON M5S 3E1, Canada
[6]Epithelial Cell Biology Laboratory, Institute of Molecular and Cell Biology Agency for Science, Technology, and Research, 61 Biopolis Drive, Singapore 138673
*Correspondence: liliana.attisano@utoronto.ca
DOI 10.1016/j.devcel.2010.03.007

SUMMARY

Several developmental pathways contribute to processes that regulate tissue growth and organ size. The Hippo pathway has emerged as one such critical regulator. However, how Hippo signaling is integrated with other pathways to coordinate these processes remains unclear. Here, we show that the Hippo pathway restricts Wnt/β-Catenin signaling by promoting an interaction between TAZ and DVL in the cytoplasm. TAZ inhibits the CK1δ/ε-mediated phosphorylation of DVL, thereby inhibiting Wnt/β-Catenin signaling. Abrogation of TAZ levels or Hippo signaling enhances Wnt3A-stimulated DVL phosphorylation, nuclear β-Catenin, and Wnt target gene expression. Mice lacking *Taz* develop polycystic kidneys with enhanced cytoplasmic and nuclear β-Catenin. Moreover, in *Drosophila*, Hippo signaling modulates Wg target gene expression. These results uncover a cytoplasmic function of TAZ in regulating Wnt signaling and highlight the role of the Hippo pathway in coordinating morphogenetic signaling with growth control.

INTRODUCTION

Animal development requires the coordination of cell patterning events with growth and proliferation signals to insure appropriate organ architecture and size. These types of developmental processes require precise cell-cell communication, which, if misregulated, can result in pathological disorders such as cancer. Secreted factors facilitate cell-cell communication and provide a mechanism for spatial and temporal control during development. Wnts comprise one such family of secreted proteins and act as morphogens to control cell fate, differentiation, and proliferation. Wnts bind to cell-surface Frizzled and LRP receptors and thereby stimulate diverse biological responses (Clevers, 2006; Nusse, 2005). At the core of the canonical Wnt pathway is the transcriptional regulator β-Catenin. In the absence of Wnt stimulation, β-Catenin levels are kept low by proteasome-mediated degradation (Aberle et al., 1997). Activation of Wnt signaling induces the hyperphosphorylation of Dishevelled (DVL), and this, via a poorly understood mechanism, ultimately leads to a rise in β-Catenin levels and to the activation of β-Catenin target genes (Clevers, 2006; Nusse, 2005). Given that aberrant activation of canonical Wnt signaling disrupts development and promotes tumorigenesis, understanding the mechanisms that normally function to restrict these signals is critical.

The precise control of organ size requires appropriate signaling via the Hippo pathway, which plays a key role in controlling cell proliferation and apoptosis (Saucedo and Edgar, 2007; Zhao et al., 2008). Central to this pathway is a kinase cascade in which the Ste20-like kinases MST1 and MST2 (Hippo/Hpo in *Drosophila*) phosphorylate and activate the NDR family kinases, LATS1 and LATS2 (Warts/Wts in *Drosophila*) (Chan et al., 2005). LATS kinases subsequently phosphorylate the transcriptional regulators TAZ and YAP (Yorkie/Yki in *Drosophila*) (Dong et al., 2007; Lei et al., 2008). Phosphorylation of TAZ and YAP promotes their interaction with 14-3-3 proteins and results in their cytoplasmic retention (Basu et al., 2003; Kanai et al., 2000). In the nucleus, TAZ and YAP can associate with a number of developmentally important proteins to mediate the transcription of genes that control cell proliferation and apoptosis, stem cell maintenance, and differentiation (Saucedo and Edgar, 2007; Zhao et al., 2008). More recently, other functions for TAZ and YAP have emerged. For example, TAZ regulates the nuclear localization of TGFβ-regulated Smad transcription factors (Varelas et al., 2008) and can regulate SCF ubiquitin ligases (Tian et al., 2007). Studies in mice have shown that Taz and Yap can have unique roles in vivo, as $Taz^{-/-}$ mice develop polycystic kidney disease (PKD) and emphysema (Hossain et al., 2007; Makita et al., 2008; Tian et al., 2007), whereas $Yap^{-/-}$ mice display embryonic lethality at embryonic day 8.5 (E8.5), with defects in yolk sac vasculogenesis, chorioallantoic attachment, and embryonic axis elongation (Morin-Kensicki et al., 2006). However, clear evidence for Taz/Yap functional redundancy has been provided by the observation

that *Taz/Yap* double-knockout mice die prior to the morula stage (Nishioka et al., 2009).

Here, we demonstrate that TAZ, an integral member of the Hippo pathway, binds DVL and negatively regulates the Wnt pathway. We show that loss of TAZ increases DVL2 phosphorylation and Wnt-dependent β-Catenin activation, resulting in enhanced cytoplasmic and nuclear β-Catenin accumulation in cell culture and in the kidneys of *Taz*-null mice. Furthermore, loss of Hippo pathway activity leads to increased nuclear TAZ and reduced TAZ-DVL binding, which results in increased Wnt-stimulated DVL2 phosphorylation, β-Catenin nuclear accumulation, and induction of Wnt-target genes. As in mammalian cells, we show that the Hippo pathway negatively regulates Wingless (Wg) signaling in *Drosophila* imaginal discs. These studies reveal a conserved function for the Hippo pathway in modulating Wnt signaling via TAZ, and provide insight into how morphogen signaling is coordinated with pathways that control tissue growth.

RESULTS

TAZ Is a Negative Regulator of Wnt/β-Catenin Signaling

To identify novel Wnt/β-Catenin pathway components, we implemented a multidimensional screening approach to query the contribution to the Wnt pathway of a focused subset of 640 genes enriched in intracellular signaling components (Barrios-Rodiles et al., 2005; Miller et al., 2009). For this, we used three mammalian cell-based high-throughput assays that included the LUMIER protein-protein interaction assay (Barrios-Rodiles et al., 2005) and two screens examining how overexpression versus siRNA-mediated gene knockdown affected Wnt3A-dependent induction of the transcriptional reporter TOPflash (Miller et al., 2009). Meta-analysis of these data uncovered the transcriptional regulator TAZ as a regulator of Wnt/β-Catenin signaling. Specifically, we observed that siRNA-mediated knockdown of TAZ enhanced Wnt3A-induced TOPflash activity, and that TAZ strongly associated with DVL2 in LUMIER (see Figure S1 available online). Accordingly, we demonstrated that RNAi-mediated knockdown of endogenous TAZ expression in HEK293T cells, using either a pool or a distinct single siRNA, enhanced TOPflash reporter activity, but not that of the nonresponsive FOPflash control reporter (Figures 1A; Figure S1C). Expression of low levels of siRNA-resistant mouse Taz rescued the siTAZ-mediated increase of TOPflash reporter activity in the human HEK293T cells, confirming the specificity of the TAZ siRNA (Figure 1B). We also examined endogenous Wnt signaling by using the Wnt-responsive breast cancer cell line, MDA-MB-231. Quantitative real-time PCR analysis revealed that knockdown of TAZ in MDA-MB-231 cells enhanced Wnt3A-induced AXIN2, NKD1, and TNFRSF19 expression (Figure 1C). Moreover, TAZ knockdown increased endogenous β-Catenin protein levels (Figure 1D) and enhanced nuclear accumulation of β-Catenin after Wnt3A stimulation (Figure 1E). Collectively, these results show that TAZ is a negative regulator of the Wnt pathway.

Taz Mutant Kidneys Display Enhanced Cytoplasmic and Nuclear β-Catenin Localization

Taz-null mice develop severe renal cysts (Hossain et al., 2007; Makita et al., 2008; Tian et al., 2007) that resemble those formed in human PKD. Excessive Wnt signaling in mouse kidneys, as the result of either ectopic expression of an activated mutant of β-Catenin or via loss of *Apc*, also yields polycystic kidney lesions (Saadi-Kheddouci et al., 2001; Sansom et al., 2005). Moreover, cysts from patients with autosomal dominant PKD (ADPKD) display a gene signature indicative of activated Wnt signaling (Lal et al., 2008). We therefore generated *Taz* mutant mice by using a genetrap (gt) line (Figure S2), and we examined the localization of β-Catenin in kidney sections from wild-type (WT) and $Taz^{gt/gt}$ mouse embryos by confocal microscopy. In $Taz^{gt/gt}$ mice, renal cysts were first detected at around E15–16, consistent with other *Taz* mutant mice (Hossain et al., 2007). Therefore, we first examined β-Catenin localization at the onset of cyst formation at E15 (Figure 2A). In epithelial structures of WT kidneys, β-Catenin was predominantly localized in junctions, although in some cells β-Catenin was also localized in the cytoplasm. In $Taz^{gt/gt}$ kidneys, β-Catenin displayed prominent cytoplasmic and nuclear localization in tubules that otherwise displayed normal morphology. Next, we analyzed cysts in E16 and E17 embryos. Unlike WT kidneys, where β-Catenin was strongly junctional, with little or no nuclear localization, $Taz^{gt/gt}$ kidneys displayed prominent cytoplasmic and nuclear localization of β-Catenin (Figure 2A). Similar redistribution of β-Catenin was also observed in E18.5 kidneys derived from a distinct *Taz*-null line (Hossain et al., 2007); data not shown). Quantitation of β-Catenin localization from a series of random images obtained from regions near the renal cortex of WT and $Taz^{gt/gt}$ kidneys revealed that from E15 to E17 ~80% of $Taz^{gt/gt}$ tubules displayed cytoplasmic and/or nuclear β-Catenin as compared to ~40%–60% of tubules from WT mice (Figure 2B). Strikingly, as the $Taz^{gt/gt}$ mutants progressed from E15 to E17, ~15% of their tubules displayed predominantly nuclear β-Catenin, whereas virtually no WT structures (1%) displayed this localization pattern. These observations demonstrate that interfering with Taz in the kidney leads to increased cytoplasmic and nuclear β-Catenin, supporting the notion that Taz is a negative regulator of the canonical WNT pathway in vivo.

TAZ Inhibits Wnt3A-Induced Phosphorylation of DVL2

To gain insight into the mechanism of the inhibitory activity of TAZ on Wnt signaling, we focused on investigating the association of TAZ with DVL that was first revealed in our LUMIER screen (Figure S1). Immunoprecipitation of Flag-tagged DVL1, DVL2, or DVL3 followed by immunoblotting for HA-tagged TAZ revealed that TAZ interacted with all three DVL isoforms, with a preference for DVL2 (Figure 3A). Endogenous TAZ and DVL2 also interacted in both MDA-MB-231 and HEK293T cells (Figure 3B; data not shown). To map the determinants of the interaction, TAZ deletion mutants were tested for interaction with DVL2 by LUMIER. This revealed that the WW domain and the carboxy-terminal PDZ-binding motif of TAZ both contribute to the association of TAZ with DVL2 (Figure 3C). Conversely, analysis of the binding of a series of DVL2 mutants to TAZ demonstrated that the PDZ domain and a PY motif located at amino acids 564–568 both contribute to the interaction (Figure 3D). Importantly, deletion of the WW domain and PDZ-binding motif of TAZ did not affect interaction with another known interactor, β-TrCP (Figure S3).

Wnt3A induces DVL phosphorylation, an event that preceeds β-Catenin stabilization and activation (Wallingford and Habas,

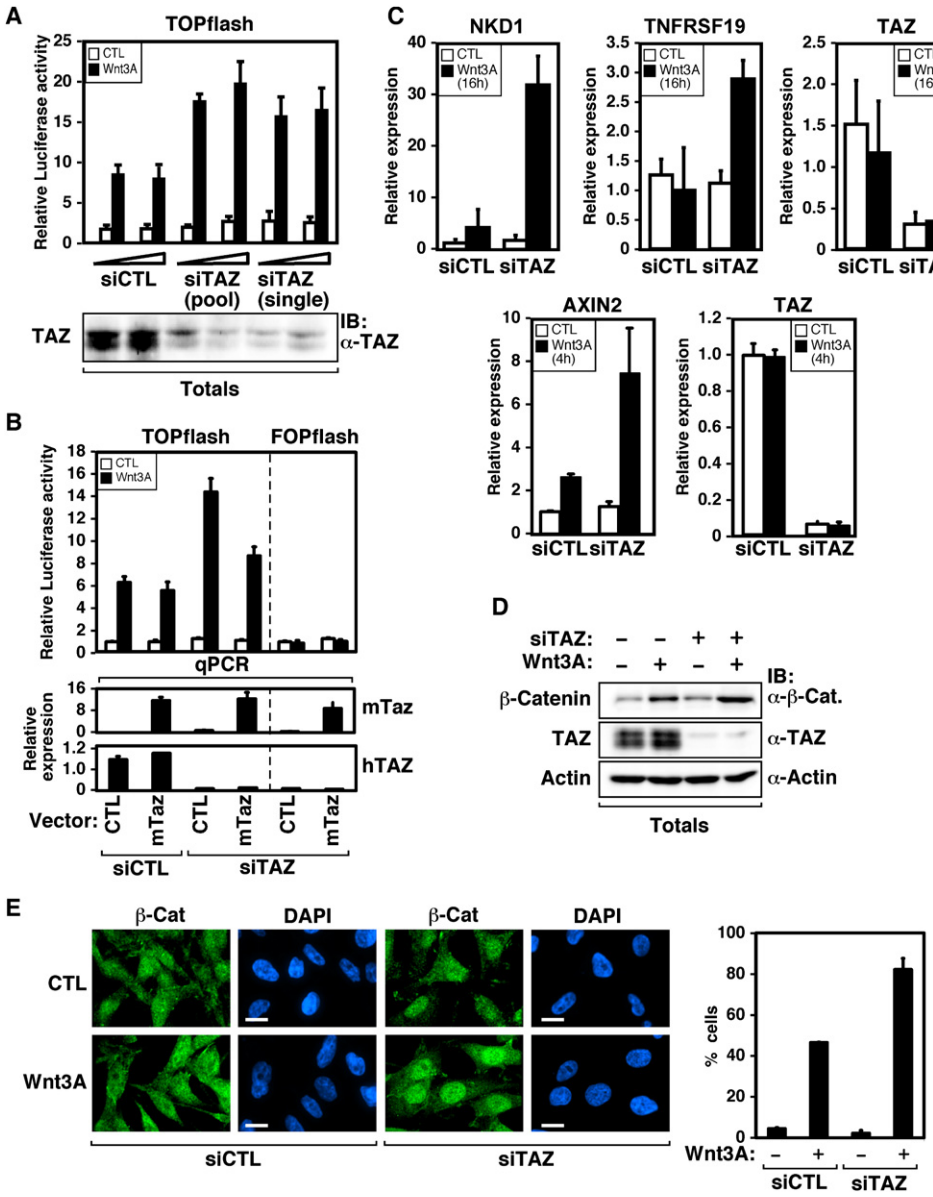

Figure 1. TAZ is a Negative Regulator of the Wnt/β-Catenin Pathway

(A) TAZ knockdown enhances Wnt3A-induced activity of the TOPflash reporter. TOPflash reporter activity was measured in HEK293T cells transfected with increasing amounts (25 nM or 50 nM) of pooled or single TAZ siRNA (siTAZ) or a scrambled control (siCTL), and then treated with control or Wnt3A-conditioned media.

(B) siRNA-resistant TAZ rescues enhanced Wnt signaling resulting from TAZ knockdown. TOPflash and FOPflash reporter activity was measured in HEK293T cells transfected with siCTL or siTAZ expressing very low levels of siRNA-resistant mouse Taz and after treatment with control of Wnt3A-conditioned media. The relative levels of mouse and human TAZ were measured by quantitative RT-PCR in parallel samples.

(C) TAZ knockdown induces Wnt3A-dependent target gene expression. The expression of NKD1, TNFRSF19, and AXIN2 was determined by qPCR from MDA-MB-231 cells transfected with siTAZ or siCTL and treated for 4 or 16 hr with control or Wnt3A-conditioned media as indicated.

(D) TAZ knockdown stabilizes β-Catenin levels. MDA-MB-231 cells were transfected with siTAZ or siCTL and treated with control or Wnt3A-conditioned media for 4 hr, and total cell lysates were subsequently analyzed for β-Catenin levels by immunoblotting.

(E) Knockdown of TAZ induces nuclear β-Catenin accumulation. MDA-MB-231 cells were transfected with siTAZ or siCTL and treated with control or Wnt3A-conditioned media for 2 hr. Cells were then analyzed for endogenous β-Catenin localization by immunofluorescent microscopy. The scale bar represents 10 μM. The percentage of cells displaying high nuclear/cytoplasmic variance of β-Catenin signal is shown. Data show that after Wnt3A treatment, siTAZ-treated cells displayed high nuclear/cytoplasmic variance ($p < 0.0001$).

2005). Therefore, we examined whether TAZ regulates DVL2 phosphorylation. Knockdown of TAZ expression in MDA-MB-231 cells increased phosphorylation of endogenous DVL2 that was further enhanced by Wnt3A stimulation (Figure 4A). CK1ε, and the highly related CK1δ, have been shown to mediate Wnt-induced DVL phosphorylation (McKay et al., 2001). Therefore,

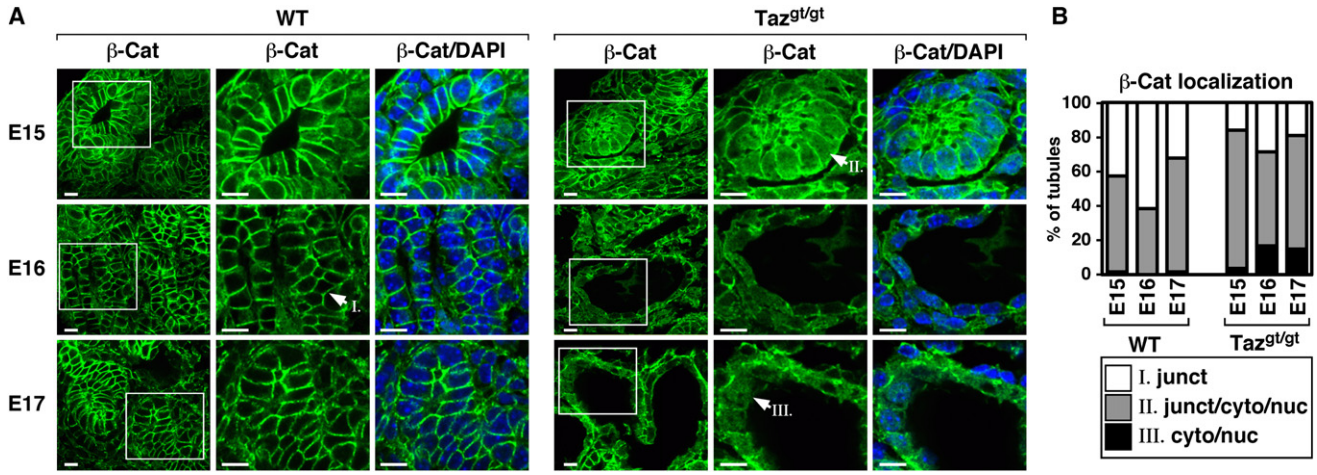

Figure 2. Mislocalization of β-Catenin in Kidney Cysts of *Taz*$^{gt/gt}$ Mouse Embryos

(A) Kidney sections from E15, E16, or E17 WT or *Taz*$^{gt/gt}$ mice were analyzed by immunostaining for β-Catenin. Higher-magnification images of boxed sections are shown. The cell nuclei were visualized by DAPI staining. The scale bar represents 10 μM.

(B) β-Catenin localization was assessed in tubules from WT and *Taz*$^{gt/gt}$ embryonic kidneys and classified as junctional (junct), junctional/cytoplasmic/nuclear (junct/cyto/nuc), or cytoplasmic/nuclear (cyto/nuc), with representative tubules marked as I, II, or III, respectively. The percentage of total tubules from E15, E16, and E17 kidneys is shown after the quantitation of 193 WT and 187 *Taz*$^{gt/gt}$ tubules.

we sought to determine whether TAZ regulates CK1δ/ε-dependent DVL2 phosphorylation. Treatment of MDA-MB-231 cells with a CK1δ/ε inhibitor, IC261 (Mashhoon et al., 2000), efficiently blocked Wnt-induced DVL phosphorylation, but resulted in only a partial inhibition of β-Catenin stabilization. This suggests the existence of both CK1δ/ε-dependent and -independent routes to β-Catenin stabilization, as has been reported previously (Bryja et al., 2007). Importantly, treatment of cells with IC261 blocked siTAZ-induced DVL2 phosphorylation, both in the presence and absence of Wnt3A treatment, and concomitantly reduced siTAZ-induced β-Catenin stabilization (Figure 4A). Similarly, targeting of endogenous CK1δ/ε with siRNAs also prevented the enhancement of DVL2 phosphorylation caused by TAZ knockdown (Figure 4B). Moreover, blocking CK1ε activity or expression with IC261 or siRNA, respectively, reversed the effect of siTAZ on Wnt3A-mediated activation of the TOPflash reporter (Figure 4C; Figure S4A). Consistent with a role for TAZ upstream of the β-Catenin destruction complex, siRNA-mediated abrogation of TAZ expression had no effect on constitutive TOPflash activity in SW480 or Colo205 colorectal cancer cells, which harbor mutations in *APC* (Figure S4B). However, RKO colon cancer cells, which retain WT *APC*, displayed increased TOPflash activity after TAZ knockdown (Figure S4B). Altogether, these results demonstrate that TAZ suppresses Wnt3A signaling by limiting the ability of CK1δ/ε to phosphorylate DVL2.

CK1δ/ε bind to DVLs (McKay et al., 2001), thus we extended our analysis to examine whether TAZ interferes with the CK1δ/ε-DVL interaction. Indeed, expression of WT TAZ inhibited the association of transfected CK1δ/ε with DVL2 (Figure 4D). Similarly, LUMIER analysis revealed that TAZ inhibited the interaction of endogenous DVL2 with luciferase-tagged CK1ε, whereas expression of the DVL2-binding mutant of TAZ (TAZ 1–393, ΔWW) did not (Figure 4E). Thus, TAZ prevents CK1δ/ε from associating with and phosphorylating DVL2. To examine the effect of the DVL-binding mutant of TAZ on Wnt signaling, we eliminated endogenous TAZ expression by using siRNA and expressed low levels of siRNA-resistant mouse Taz. Analysis of TOPflash activation showed that WT Taz rescued the siTAZ-mediated increase in TOPflash reporter activity, whereas the DVL2-binding mutant (Taz 1-393, ΔWW) did not (Figure 4F). Of note, the Taz S89A mutant, which is unable to bind to 14-3-3 proteins and is localized predominantly in the nucleus, also failed to rescue siTAZ enhancement of TOPflash activation (Figure 4F). Altogether, these results demonstrate that TAZ functions in the cytoplasm to downregulate Wnt/β-Catenin signaling by binding DVL2 and preventing the phosphorylation by CK1δ/ε.

Hippo Signaling Promotes the Association of Cytoplasmic TAZ with DVL2 to Downregulate Wnt/β-Catenin Signaling

The activity of TAZ in restricting Wnt signaling suggests that pathways that regulate TAZ may, in turn, modulate Wnt/β-Catenin activity. In *Drosophila*, the Hpo/Wts kinase pathway regulates the localization and activity of the TAZ/YAP homolog Yki, and the orthologous mammalian MST/LATS pathway has been similarly implicated in regulating TAZ and YAP function (Saucedo and Edgar, 2007; Zhao et al., 2008). Therefore, we examined whether this pathway influences TAZ function in Wnt/β-Catenin signaling. In mammals, two Hpo kinase homologs, MST1 and MST2, are upstream activators of the two Wts kinase homologs, LATS1 and LATS2, which phosphorylate TAZ and YAP. Indeed, LATS2 phosphorylates TAZ on serine 89 (Lei et al., 2008), and we confirmed that LATS1 also phosphorylated TAZ on serine 89 (Figure S5). In addition, coexpression of the LATS1 activators MST1 or MST2 further increased TAZ phosphorylation (Figure S5), and endogenous LATS1 and TAZ interacted in MDA-MB-231 cells (Figure 5A). To examine if MST/LATS regulates Wnt signaling, we employed siRNA to knock down LATS1, LATS2, MST1, or MST2 and examined activation of the TOPflash reporter in HEK293T cells. Efficient knockdown was confirmed

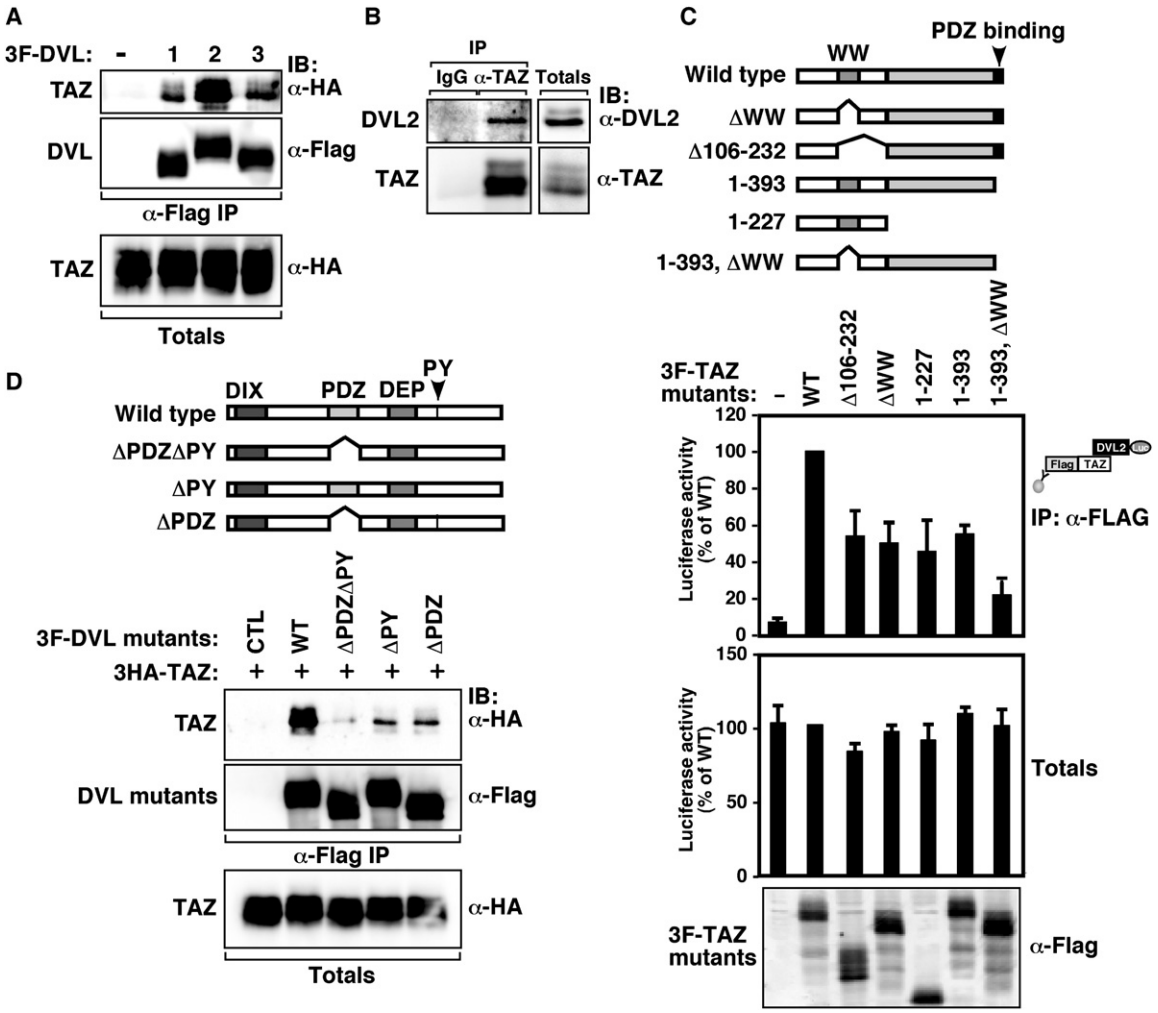

Figure 3. TAZ Binds to Dishevelled

(A) TAZ interacts with DVLs. HEK293T cells were transfected with HA-TAZ and Flag-DVL1, -2, or -3. After anti-Flag immunoprecipitation, the presence of TAZ was detected by anti-HA immunoblotting.

(B) Interaction of endogenous TAZ and DVL2. Cell lysates from MDA-MB-231 cells were subjected to immunoprecipitation with anti-TAZ antibody or control IgG, and the presence of DVL2 was examined by anti-DVL2 immunoblotting.

(C) DVL2 interacts with the WW domain and PDZ-binding motif of TAZ. HEK293T cells were cotransfected with the indicated Flag-TAZ WT or mutant constructs and DVL2 tagged with Firefly luciferase. Cell lysates were subjected to anti-Flag immunoprecipitation, and the presence of DVL2 was assessed by luciferase assay.

(D) TAZ interacts with the PY motif and PDZ domain of DVL2. HEK293T cells were cotransfected with the indicated Flag-DVL2 WT or mutant constructs and HA-TAZ. Cell lysates were subjected to anti-Flag immunoprecipitation, and the presence of TAZ was assessed by anti-HA immunoblotting.

by immunoblotting or real-time PCR (Figures 5B and 5C; data not shown). These analyses revealed that targeting any of the LATS or MST kinases enhanced TOPflash activity, with the greatest effects being observed upon knockdown of either LATS1 or MST2 (Figure 5B). Because knockdown of both LATS1 and LATS2 or both MST1 and MST2 did not further enhance TOPflash signaling, our results suggest that, in HEK293T cells, MST2-LATS1 is the predominant kinase cascade regulating Wnt. Consistent with our results, a genome-wide siRNA screen also found that knockdown of LATS1 increased Wnt-induced reporter activity (DasGupta et al., 2005). We next determined the expression of the endogenous Wnt target gene, AXIN2, in MDA-MB-231 cells. Similar to siTAZ (Figure 1C), siRNA-mediated knockdown of LATS1 or MST2 increased Wnt3A-dependent AXIN2 expression (Figure 5C).

We next examined the effects of overexpressing MST/LATS, which phosphorylates TAZ and thereby drives binding to 14-3-3 proteins and cytoplasmic retention of TAZ (Kanai et al., 2000). This analysis revealed that overexpression of LATS1 or MST2 alone reduced TOPflash, but not FOPflash, reporter activity (Figure 5D; Figure S5B). Further reductions were observed when LATS1 was coexpressed together with a WT, but not a kinase-dead (K56R), version of MST2, its upstream activator (Figure 5D). Importantly, inhibition of TOPFlash activation by MST/LATS was suppressed by TAZ knockdown (Figure 5E), consistent with TAZ functioning downstream of MST/LATS in

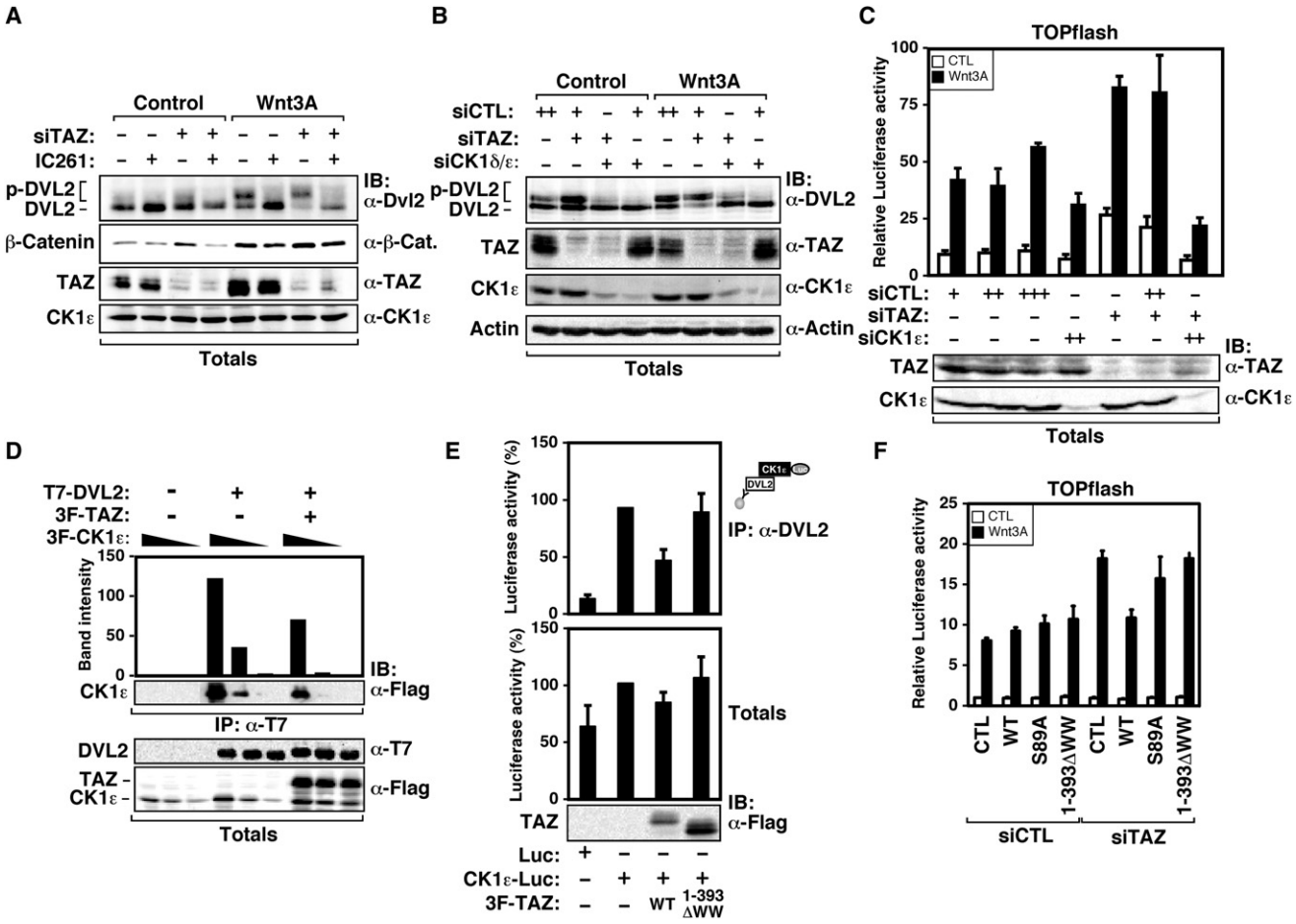

Figure 4. TAZ Inhibits DVL2 Phosphorylation by CK1δ/ε

(A and B) TAZ knockdown induces CK1δ/ε-mediated DVL2 phosphorylation. (A) MDA-MB-231 cells were transfected with siCTL or siTAZ, treated with or without the CK1δ/ε inhibitor IC261 for 1 hr, and then treated with control or Wnt3A-conditioned media for 4 hr. Cell lysates were then analyzed by immunoblotting with the indicated antibodies. (B) MDA-MB-231 cells were transfected with 50 nM siCTL or siTAZ, or 50 nM of total siRNA comprised of combinations of TAZ, CK1δ, and CK1ε, as indicated. Cells were treated with control or Wnt3A-conditioned media for 4 hr, lysed, and analyzed by immunoblotting.

(C) CK1ε knockdown inhibits the enhanced TOPflash activity caused by TAZ knockdown. TOPflash activity was measured in HEK293T cells transfected with the indicated siRNAs, and then treated with control or Wnt3A-conditioned media. Data from a representative experiment are plotted as the mean of three replicates plus standard deviation. Knockdown was confirmed by immunoblotting.

(D) TAZ overexpression inhibits the interaction of DVL2 with CK1ε. HEK293T cells were transfected with T7-DVL2, Flag-TAZ, and decreasing amounts of Flag-CK1ε. Interactions were detected by anti-T7 immunoprecipitation followed by anti-Flag immunoblotting. CK1ε levels were quantitated with ImageQuant software (top panel).

(E) A DVL2-binding mutant of TAZ does not inhibit the interaction of DVL2 with CK1ε. Cells were transfected with Firefly luciferase (Luc) or with CK1ε tagged with Firefly luciferase (CK1-Luc) along with Flag-tagged WT or mutant (1–393, ΔWW) TAZ. The interaction between DVL2 and CK1ε was detected by immunoprecipitation of endogenous DVL2 followed by a luciferase assay.

(F) WT TAZ, but not the DVL2-binding mutant nor the nuclear-localized TAZ-S89A, rescue the enhanced Wnt signaling resulting from TAZ knockdown. TOPflash reporter activity after treatment with control or Wnt3A-conditioned media was measured in HEK293T cells transfected with siCTL or siTAZ expressing low levels of siRNA-resistant mouse WT Taz, Taz (1-393, ΔWW), or Taz (S89A). Data from a representative experiment are plotted as the mean of three replicates plus standard deviation.

mediating this effect. We next examined the localization of TAZ and β-Catenin in the absence of LATS1. As expected, knockdown of LATS1 in MDA-MB-231 cells led to prominent nuclear localization of TAZ, whereas, in control conditions, TAZ was distributed throughout the cell (Figure 6A). Parallel examination of the localization of β-Catenin revealed increased nuclear accumulation of β-Catenin in siLATS1-transfected cells treated with Wnt3A (Figure 6A). These results suggest that MST/LATS-mediated phosphorylation of TAZ inhibits Wnt/β-Catenin signaling by retaining TAZ in the cytoplasm, where it inhibits DVL activation. To explore this further, we examined whether the TAZ-DVL2 interaction is modulated by LATS1. Indeed, in the absence of LATS1, the association of TAZ with endogenous DVL2 was reduced (Figure 6B; Figure S6) and concomitantly led to increased levels of phosphorylated DVL2 (Figure 6C). Collectively, these data indicate that Hippo signaling regulates

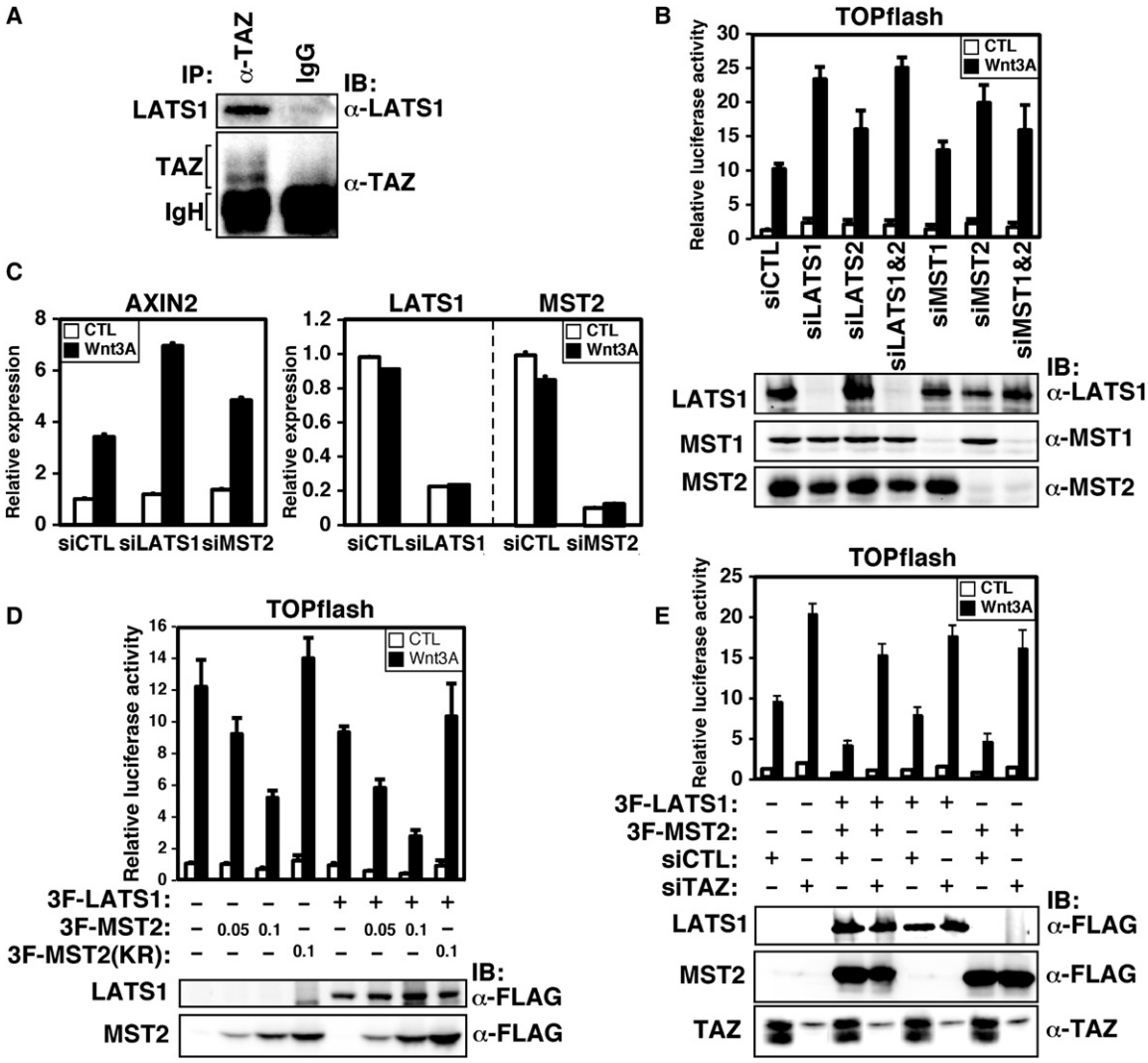

Figure 5. The MST/LATS Pathway Inhibits Wnt/β-Catenin Signaling

(A) Interaction of endogenous TAZ and LATS1. Cell lysates from MDA-MB-231 cells were subjected to immunoprecipitation with anti-TAZ antibody or control IgG, and the presence of LATS1 was detected by immunoblotting.

(B) Loss of MST/LATS expression enhances Wnt3A-induced transcriptional responses. TOPflash reporter activity was measured in HEK293T cells transfected with siRNAs targeting LATS1, LATS2, MST1, or MST2, as indicated, and then incubated with control or Wnt3A-conditioned media. Data from a representative experiment are plotted as the mean of three replicates plus standard deviation. Immunoblots from total cell lysates were performed to confirm knockdown. Knockdown of LATS2 was confirmed by RT-PCR (data not shown).

(C) MST/LATS knockdown enhances Wnt3A-dependent AXIN2 expression. The expression of AXIN2 was determined by qPCR from MDA-MB-231 cells transfected with siCTL, siLATS1, or siMST2, and then treated with control or Wnt3A-conditioned media for 4 hr.

(D and E) (D) MST/LATS overexpression inhibits Wnt3A-induced TOPflash activity. HEK293T cells were cotransfected with the TOPflash reporter together with LATS1 and 0.05 μg or 0.1 μg MST2 or 0.1 μg MST2 (KR) as indicated, and then treated with control or Wnt3A conditioned media. (E) TAZ knockdown suppresses the inhibitory effect of MST/LATS overexpression on Wnt signaling. HEK293T cells were transfected with the TOPflash reporter, siCTL or siTAZ, and with LATS1 and MST2, and then treated with control or Wnt3A-conditioned media. (D and E) Data from representative experiments are plotted as the mean of three replicates plus standard deviation.

a cytoplasmic function for TAZ in inhibiting CK1δ/ε-mediated DVL2 phosphorylation, to modulate downstream Wnt signaling events.

The *Drosophila* Hippo Pathway Regulates Wingless/Armadillo Signaling

In *Drosophila*, the Hippo pathway limits organ size, and loss of the Hippo kinase cascade results in excessive proliferation of imaginal discs, the adult limb precursors (Harvey et al., 2003; Huang et al., 2005; Xu et al., 1995). A key role for the Wnt-family ligand Wg as a morphogen that drives development and patterning in imaginal discs has been well established (Zecca et al., 1996). Therefore, to examine modulation of Wnt signaling by the Hippo pathway in vivo, we employed clonal analysis in *Drosophila*, which possess a single Hpo and a single Wts kinase. First, we confirmed that Yki, the *Drosophila* homolog of TAZ,

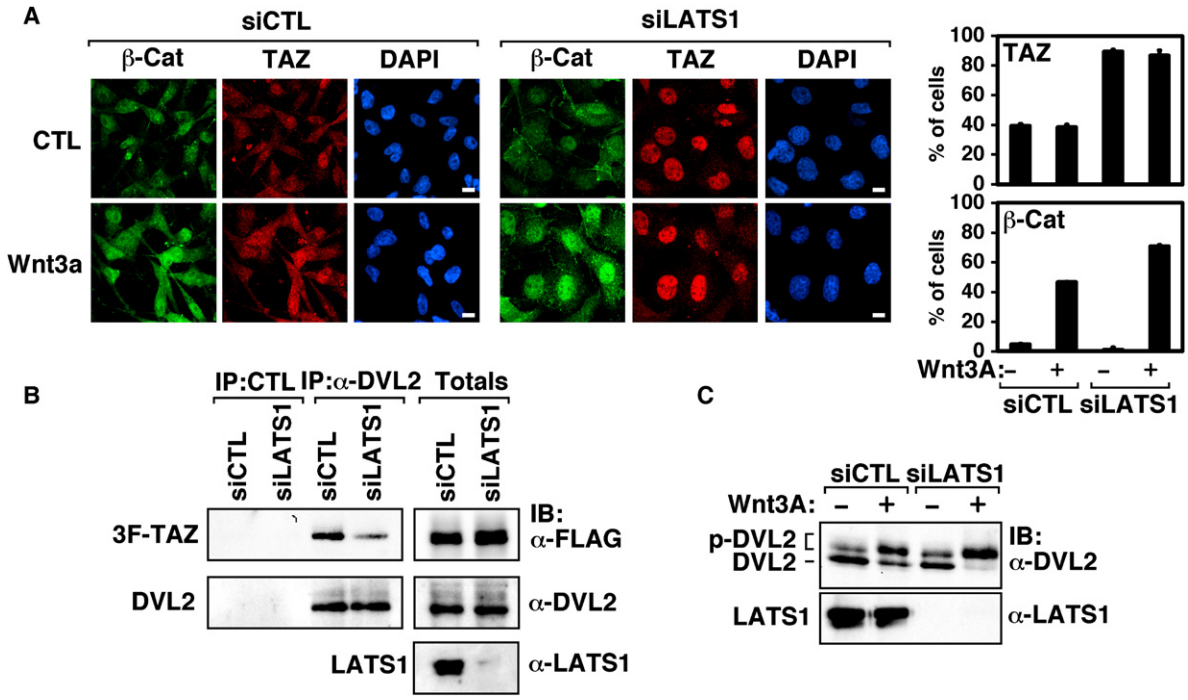

Figure 6. LATS1 Activity Promotes a Cytoplasmic Role for TAZ in the Inhibition of Wnt/β-Catenin Signaling

(A) Abrogation of LATS1 expression induces TAZ nuclear accumulation and stimulates nuclear β-Catenin localization in response to Wnt3A. MDA-MB-231 cells were transfected with siCTL or siLATS1, and then treated with control or Wnt3A-conditioned media for 2 hr. Cells were then analyzed for endogenous TAZ and β-Catenin localization by immunofluorescent microscopy. The cell nuclei were visualized by DAPI staining. The scale bar represents 10 μM. The percentage of cells displaying high nuclear/cytoplasmic variance of β-Catenin signal is shown. Data show that after Wnt3A treatment, siLATS1-treated cells displayed high nuclear/cytoplasmic variance ($p < 0.0001$).

(B) TAZ binding to DVL2 is disrupted in the absence of LATS1. MDA-MB-231 cells stably expressing Flag-TAZ were transfected with siCTL or siLATS1. Endogenous DVL2 was immunoprecipitated from cell lysates with an anti-DVL2 Fab (see Figure S6), and associated TAZ was analyzed by immunoblotting.

(C) Abrogation of LATS expression enhances Wnt3A-dependent DVL2 phosphorylation. MDA-MB-231 cells were transfected with siCTL or siLATS1 and treated with control or Wnt3A-conditioned media for 4 hr. Cell lysates were then analyzed by immunoblotting with the indicated antibodies.

interacts with *Drosophila* Dishevelled (Dsh) (Figure S7A). As observed for the mammalian counterparts, mapping of the Dsh-Yki interaction revealed that the PDZ domain and a PY motif from amino acids 521–525 of Dsh were critical for Yki binding. The fact that Yki lacks a carboxy-terminal PDZ-binding motif suggests that Yki contains an internal PDZ-binding domain similar to that which has been described for other regulators of the Wnt pathway (London et al., 2004; Wong et al., 2003). Next, we generated *hpo* and *wts* mutant clones in third-instar wing imaginal discs by using Flp-mediated mitotic recombination, a site-directed recombination method that generates clonal mutant tissue adjacent to WT twin spot tissue (Xu and Rubin, 1993). Wg is expressed along the dorsal/ventral (D/V) boundary in the wing pouch (see Figures S7D and S7E), and the highest levels of Armadillo (Arm), the *Drosophila* β-Catenin ortholog, are typically observed adjacent to this region (Riggleman et al., 1990). In clones lacking either *wts* or *hpo*, as marked by the absence of GFP, we observed increased Arm protein levels extending away from the Wg stripe at the D/V boundary, whereas adjacent GFP-expressing WT twin spots did not (Figure 7A; Figure S7C). Of note, Arm levels in clones of *wts*, the direct Yki kinase, were much higher than those observed in clones of *hpo*, indicating that Wts activity is subject to additional regulatory inputs, as previously suggested (Harvey et al., 2003; Wu et al., 2003). In addition, the increase in Arm levels was much less in both *wts* and *hpo* mutant clones at the boundary with WT tissue, an effect that was much more evident as clones extended away from the D/V boundary and the source of Wg (Figure 7A; Figure S7C). This might suggest that WT tissue influences Hippo pathway activity in a non-cell-autonomous manner to regulate Arm levels, although the precise nature of these signals is unclear.

To confirm that increased Arm levels were not due to increased Wg ligand, we examined Wg expression levels in *hpo* and *wts* mutant clones and found no noticeable changes in Wg levels in the wing pouch region (Figures S7D and S7E), as previously described (Cho et al., 2006). Thus, the increase in Arm levels is not due to alterations in expression of the Wg ligand. We next examined a Wg/Arm target, Distal-less (Dll), which is normally expressed ~20 cells from the D/V boundary (Zecca et al., 1996). In *wts* mutant clones, Dll levels were increased and extended farther from the D/V boundary (Figure 7B) compared to the WT twin spot tissue. Interestingly, increased Dll levels were most evident in regions distant from the D/V boundary, where Wg levels are low. Similarly, we also observed that Achaete, another Wg target that is expressed in

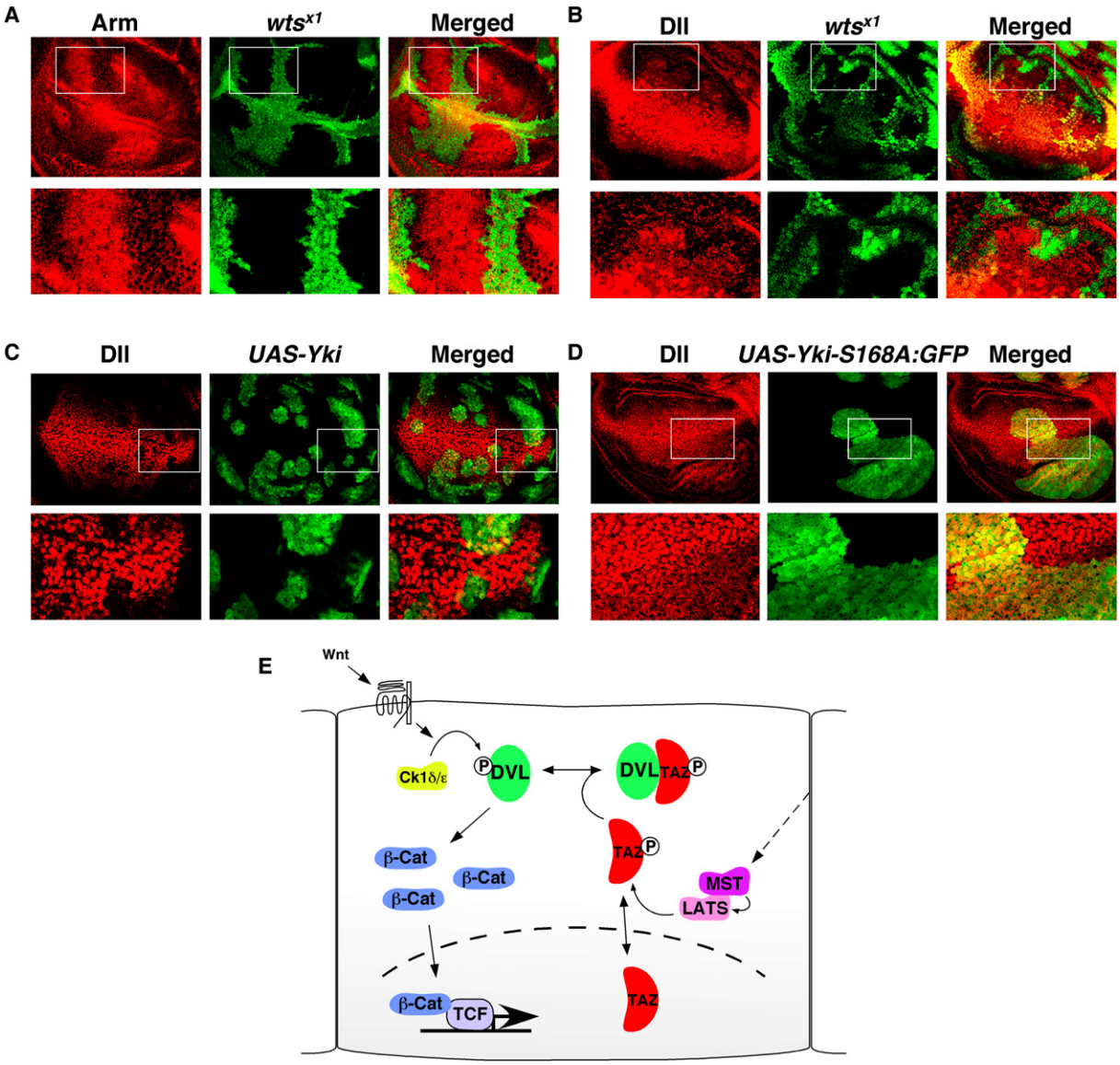

Figure 7. The *Drosophila* Hippo Pathway Inhibits Wingless Signaling

(A) *wts* mutant clones have enhanced Arm levels near the D/V boundary in wing imaginal discs. Third-instar wing imaginal discs containing *wts*^{x1} clones, marked by the absence of GFP, were immunostained with an anti-Arm antibody. A higher-magnification image of the boxed section highlights a clone with enhanced Arm levels.

(B) The levels of the Wg target, Dll, are enhanced in the outer regions of the wing pouch in *wts* mutant clones. Third-instar wing imaginal discs containing *wts*^{x1} clones were immunostained with an anti-Dll antibody. A higher magnification image of the outer wing pouch, a region at which Wg levels are low, highlight the increased levels of Dll in the absence of *wts*.

(C) The levels of the Wg target, Dll, are decreased in WT Yki-expressing tissue. Third-instar wing imaginal discs expressing WT Yki were immunostained with an anti-Dll antibody. A higher-magnification image highlights the decreased levels of Dll.

(D) The levels of the Wg target, Dll, are maintained in Yki-S168A-expressing tissue. Third-instar wing imaginal discs expressing the nuclear-localized Yki-S168A mutant were immunostained with an anti-Dll antibody. A higher-magnification image highlights the unaltered levels of Dll.

(E) A model for Hippo pathway-mediated inhibition of Wnt signaling via TAZ. The Hippo pathway kinases induce the cytoplasmic localization of TAZ, allowing for an enhanced interaction between TAZ and DVL. TAZ's interaction with DVL inhibits CK1δ/ε binding and Wnt3A-induced DVL phosphorylation, thereby preventing Wnt3A-induced transcriptional responses. Thus, the Hippo pathway can limit responses to Wnt signals to modulate Wnt-regulated processes.

a more restricted region along the D/V boundary, was also increased and extended farther from the D/V boundary in *wts* mutant clones (Figure S7B).

Finally, we examined whether the Hpo/Wts target Yki regulates Wg signaling. *yki* mutant clones are very small, making analysis of Wg responses difficult. Therefore, we examined Dll levels in tissues expressing a WT *UAS-Yki* transgene (Huang et al., 2005). This revealed that ectopic expression of WT Yki resulted in decreased expression of the Wg target Dll (Figure 7C). To assess whether this effect results from the nuclear

or cytoplasmic roles of Yki, we also examined Dll expression in clones bearing a *UAS-Yki(S168A):GFP* transgene. Wts is unable to efficiently phosphorylate this mutant of Yki, which leads to the localization of Yki primarily in the nucleus (Dong et al., 2007; Oh and Irvine, 2008). Although this *Yki(S168A):GFP* transgene, which expresses a mutant of Yki with reduced cytoplasmic function, has been shown to yield lower levels of protein than the WT *UAS-Yki* transgene we used for this study (Oh and Irvine, 2008), the overgrowth phenotype is similar, indicating that the nuclear function of Yki(S168A):GFP is comparable to that of the WT Yki. We found that Dll levels were unchanged in the Yki(S168A)-expressing clones (Figure 7D), suggesting that cytoplasmic Yki inhibits Wg signaling. Altogether, our results indicate that the Hippo pathway modulates the sensitivity of the cellular response to morphogens by functioning as a conserved negative regulator of Wnt/β-Catenin signaling.

DISCUSSION

The Hpo/Wts kinase cascade has emerged as a key regulator of tissue growth and patterning (Saucedo and Edgar, 2007; Zhao et al., 2008). This kinase cascade, which in vertebrates is represented by MST and LATS, respectively, converges on the transcriptional regulator Yorkie in *Drosophila*, or the vertebrate homologs, TAZ and YAP. Recent studies have focused on the transcriptional roles for Yorkie, TAZ, and YAP in controlling growth and cell fate choice. However, these proteins are also found in the cytoplasm, where TAZ has been shown to associate with the plasma membrane and actin cytoskeleton (Kanai et al., 2000). TAZ cytoplasmic localization is mediated by LATS-dependent phosphorylation of serine 89, which drives binding to the cytoplasmic retention factor, 14-3-3 (Kanai et al., 2000). Altogether, these findings raised the possibility that TAZ has cytoplasmic functions. Here, we demonstrate that one such function is to constrain Wnt signaling by inhibiting CK1δ/ε-mediated DVL phosphorylation (see model, Figure 7E). Although the ability of CK1δ/ε to phosphorylate DVL has been well established, the precise role of this event in Wnt signaling remains to be fully understood. In our studies, we observed that CK1δ/ε-independent signaling can contribute to Wnt-induced β-Catenin stabilization. Nevertheless, our data clearly show that DVL phosphorylation and Wnt pathway activation caused by the loss of TAZ expression requires CK1δ/ε. We show that abrogation of LATS expression, which leads to the nuclear accumulation of TAZ, reduced TAZ-DVL interaction, enhanced DVL phosphorylation, and promoted Wnt pathway activation in cells. Furthermore, we show that loss of *hpo* or *wts* function or enhanced expression of *yki* in *Drosophila* wing imaginal discs also modulates Wnt signaling. Thus, by promoting the cytoplasmic localization of TAZ, the Hippo pathway not only prevents nuclear TAZ activity, as previously proposed (Kanai et al., 2000; Lei et al., 2008), but also leads to inhibition of Wnt signaling by antagonizing DVL activation. Here, we have focused our studies on TAZ, but it will be interesting to determine whether the related protein, YAP, has a similar activity in the Wnt pathway. Indeed, functional redundancy is suggested by the *Taz/Yap* double-knockout mice, which display early embryonic lethality (Nishioka et al., 2009).

Wnts are known to act throughout mammalian kidney development (Merkel et al., 2007), and hyperactivation of Wnt/β-Catenin signaling causes severe kidney defects. For example, loss of Apc function results in nuclear β-Catenin accumulation that leads to cystic kidneys (Sansom et al., 2005), and transgenic mice expressing an activated mutant of β-Catenin also develop cysts (Saadi-Kheddouci et al., 2001). *Taz* mutant mice also develop polycystic kidneys (Hossain et al., 2007; Makita et al., 2008; Tian et al., 2007), and we found increased cytoplasmic and nuclear β-Catenin in both cystic and precystic regions of $Taz^{gt/gt}$ kidneys, indicating Wnt pathway activation. Moreover, cysts formed in humans with ADPKD, caused by mutations in PC1 or PC2, display a gene expression profile consistent with Wnt pathway activation (Lal et al., 2008). β-Catenin associates with PC1 (Lal et al., 2008), and TAZ has been proposed to indirectly regulate the activity of PC2 via the SCF ubiquitin ligase β-TrCP (Tian et al., 2007). We confirmed that TAZ and TAZ (1–393, ΔWW), the DVL-binding mutant that cannot rescue the effect of loss of TAZ on Wnt signaling, both interact with β-TrCP (Figure S3). Thus, we conclude that TAZ modulates Wnt signaling via direct regulation of DVL; however, TAZ may also function indirectly to regulate the PC complex via β-TrCP. Whether TAZ may have other additional roles in Wnt signaling remains to be determined. Altogether, these results suggest that, in the kidney, TAZ restricts canonical Wnt signaling that otherwise would disrupt tubule morphogenesis and the formation of cysts.

Defects in cilia are also known to be involved in the pathogenesis of PKD. Indeed, recent analyses of *Taz* mutant kidneys have revealed that Taz localizes to cilia, and that cystic regions in $Taz^{-/-}$ kidneys have underdeveloped cilia (Hossain et al., 2007). Interestingly, primary cilia have recently been implicated in restraining Wnt signaling (Corbit et al., 2008), and DVL has been reported in cilia (Park et al., 2008). These findings raise the intriguing possibility that TAZ may link suppression of DVL activation in the kidney to ciliogenesis. Of note, we have found no evidence that the MDA-MB-231 breast cancer cells used in this study possess cilia (data not shown), indicating that cilia, per se, are not required for TAZ inhibition of Wnt signaling. Nevertheless, it will be interesting to examine the relationship between TAZ regulation of ciliogenesis and DVL modulation in kidney epithelia.

The development of multicellular organisms requires cell-cell communication and the coordinated action of distinct signaling pathways for proper patterning of the body and organs. In the *Drosophila* wing imaginal disc, the Wg morphogen gradient coordinates the expression of an array of developmentally important genes (Zecca et al., 1996). Our studies reveal that the Hippo pathway functions to restrain Wg signaling, and that loss of *hpo* or *wts* increases the levels of Arm (β-Catenin) outside the normal expression domain and enhances expression of Wg target genes, particularly at a distance from the Wg source. Thus, Hippo pathway activation may, in effect, serve to restrain the sensitivity of cells to Wg signals, thus sharpening the Wg response gradients to promote appropriate tissue patterning events. How the Hippo kinase cascade is regulated by upstream pathways remains unclear. However, genetic studies place a protocadherin, Fat, and an ERM domain protein, Expanded, upstream of Hpo/Wts kinases (Bennett and Harvey, 2006; Cho et al., 2006; Hamaratoglu et al., 2006; Silva et al., 2006; Willecke et al., 2006). Furthermore, and in accordance with our analysis of

hpo and *wts* mutants, *fat* and *expanded* mutants display enhanced Wg target gene expression independent of Wg ligand production (Tyler and Baker, 2007). Our results suggest that this occurs via a direct molecular link. In this regard, it is intriguing to note that mice null for *Fat4*, a mammalian homolog of *Drosophila fat*, also develop polycystic kidneys (Saburi et al., 2008). Direct communication between the Hippo and Wnt pathways may thus be an ancient mechanism that coordinates morphogen signaling with tissue growth control in animals.

We showed that TAZ inhibits Wnt signaling via DVL, providing for a direct molecular link between the Hippo and Wnt signaling pathways. Other studies in *Drosophila* have implicated the Hippo pathway as a positive regulator of Notch signaling (Meignin et al., 2007; Yu et al., 2008), and we previously showed an essential role for TAZ in mediating TGFβ-dependent Smad signaling (Varelas et al., 2008). Furthermore, TAZ is induced by BMP signaling to regulate mesenchymal cell differentiation (Hong et al., 2005). Altogether, these studies suggest a critical and direct role for TAZ in integrating signals from numerous morphogen signaling pathways.

EXPERIMENTAL PROCEDURES

Constructs and siRNAs

LATS1, LATS2, MST1, MST2, DVL, CK1ε, Dsh, and Yki constructs were generated by PCR and were either triple FLAG-, triple HA-, or Firefly luciferase-tagged in a pCMV5 vector. TAZ and TAZ mutant cDNA constructs were described previously (Varelas et al., 2008). siGENOME pools of siRNAs (written in the 5′ to 3′ direction) were purchased from Dharmacon, with the following exceptions: TAZ single-siRNA (ACGUUGACUUAGGAACUUU); control (Scrambled TAZ) (UAGUACUGUUACUGGCAUU); and control (invS3) (GGGC AAGACGAGCGGGAAG).

Transfection, Reporter Assays, and Real-Time Quantitative Reverse Transcription PCR

HEK293T cells were transfected with calcium phosphate or with Lipofectamine 2000 (Invitrogen), and MDA-MB-231 cells were transfected with Dharmafect 4 (Dharmacon). For reporter assays, the HEK293T cells were seeded in poly-L-lysine-coated 24-well dishes and transfected with cDNAs or siRNAs, pCMV-β-galactosidase, and either TOPflash or FOPflash reporters. For transcriptional assays, 24 hr after transfection the cells were treated with control or Wnt3A-conditioned medium for 16 hr. Luciferase activity in cell lysates was determined and normalized to β-galactosidase activity as previously described (Labbe et al., 2007). Unless otherwise indicated, siRNAs were used at a concentration of 50 nM, and cells were lysed 48 hr after transfection. The quantitation of AXIN2 gene expression by quantitative PCR (qPCR) has been described previously (Labbe et al., 2007). The ΔCT values were obtained by comparing the amplification of the target DNA to that of GAPDH. The quantitiation of *NKD1* and *TNFRSF19* gene expression was qPCR was performed with the following primers (written in the 5′ to 3′ direction): NKD1 Forward, TGAGAAGAAGATGGAGAGAGTGAGCGA; NKD1 Reverse, GGTGACCTTG CCGTTGTTGTCAAA; TNFRSF19 Forward, GGAGTTGTCTAAGGAATGTGG; TNFRSF19 Reverse, GCTGAACAATTTGCCTTCTG.

Except where otherwise stated, all graphed data are shown as the mean of three independent biological replicates plus standard error of the mean (SEM). All representative experiments shown were reproduced a minimum of three times.

Immunoprecipitation, LUMIER, and Immunoblotting

Immunoprecipitation (IP) and immunoblotting (IB) were carried out with the following antibodies: Flag (Sigma #F3165; 1 μg/IP, 1:2000 IB); T7 (Novagen #69522-3; 1 μg/IP, 1:10,000 IB); HA (Roche #11867431001; 1:1000 IB); TAZ (BD Biosciences #560235; 3 μg/IP, 1:1000 IB); TAZ (Novus #NB600-220; 1:1000 IB); CK1ε (BD Biosciences #610445; 1:2000 IB); β-Catenin (BD Biosciences #610153; 1:1000 IB); Actin (Sigma # A2066; 1:2000 IB); DVL2 (Cell Signaling Technology #3224; 1:1000 IB); LATS1 (Bethyl #A300-478A; 1:1000 IB); MST1 (BD biosciences #77120; 1:1000 IB); MST2 (Novus #NB100-79800; 1:1000 IB). LUMIER experiments were performed as previously described (Barrios-Rodiles et al., 2005; Varelas et al., 2008). All graphed data are shown as the mean of three independent biological replicates plus SEM. For DVL2 IP, a phage display-derived antibody (Fellouse et al., 2007) selected against human DVL2 was generated, and then validated for its specificity and pull-down efficiency (Figure S6). The antibody was biotin labeled, and then bound in excess to streptavidin-conjugated magnetic beads (Promega #Z5481) that were subsequently blocked with excess free biotin. The antibody-conjugated beads were then used for immunoprecipitation of endogenous DVL2 from cell lysates. Biotin-blocked, streptavidin-conjugated magnetic beads were used as a control.

Immunofluorescence

For immunofluorescent analysis of cell cultures, cells were washed with PBS, and then fixed with 4% paraformaldehyde. Cells, permeabilized with 0.2% Triton X-100 in PBS, were blocked with 2% BSA-PBS prior to the addition of primary antibodies: mouse anti-β-Catenin antibody (BD Biosciences #610153; 1:1000 in 2% BSA-PBS); rabbit-anti-β-Catenin antibody (Sigma #C2206; 1:1000 in 2% BSA-PBS); or mouse anti-TAZ antibody (BD Biosciences #560235; 1:500 in 2% BSA-PBS). Secondary antibodies used include: donkey anti-mouse Alexa Fluor 488 (Invitrogen #A21202; 1:500 in 2% BSA-PBS) and donkey anti-rabbit Alexa Fluor 555 (Invitrogen #A31572; 1:500 in 2% BSA-PBS). Cell nuclei were visualized by DAPI staining. Quantitatition of β-Catenin and TAZ nuclear/cytoplasmic localization was performed by using Image J software. Briefly, tiff images were imported into Image J, and, by using DAPI staining to mark the cell nuclei, the variance of nuclear to cytoplasmic β-Catenin or TAZ signal was measured for individual cells. The mean variance was calculated from a minimum of 310 total cells from 3 different experiments (with at least 91 and 100 cells counted from each of the control and Wnt3A-treated experiments, respectively). Cells were then grouped as low or high nuclear/cytoplasmic depending on whether they fell below or above the mean variance of the Wnt3A-treated siCTL cells, respectively. An unpaired two-tailed t test was used to determine the statistical significance. For mouse kidney analysis, E15, E16, or E17 kidneys were fixed overnight at 4°C in 4% PFA. Samples were then dehydrated, embedded in paraffin, and sectioned at 5 μM. Sections were boiled in sodium citrate (pH 6.0), incubated with β-Catenin antibody (BD Biosciences #610153; 1:500), and subsequently stained with donkey anti-mouse Alexa 555 antibody (Invitrogen #A31570; 1:500). The localization of β-Catenin within the tubules was examined and scored by using a double-blind analysis, and then grouped as junctional (I), juntional/cytoplasmic/nuclear (II), or cytoplasmic/nuclear (III). For the analysis of *Drosophila* tissues, wing imaginal discs were dissected in PBS with protease inhibitors and fixed/permeabilized in 4% paraformaldehyde with 0.3% Triton X-100. The samples were then incubated with the following primary antibodies: mouse anti-Armadillo (Development Studies Hybridoma Bank #N2-7A1; 1:250), rabbit anti-Distal-less (Sean Carroll; 1:100), mouse anti-Achaete (Development Studies Hybridoma Bank; 1:10), or mouse anti-Wingless (Development Studies Hybridoma Bank #4D4; 1:200). The secondary antibodies used were donkey anti-mouse Alexa 555 (Invitrogen #A31570; 1:500) or donkey anti-rabbit Alexa 555 (Invitrogen #A31572; 1:500). Images were captured using a spinning disk confocal (Leica) or a confocal microscope (Nikon).

Drosophila Genetics

Drosophila mutant clones were generated by FLP-FRT-mediated recombination with wts^{x1}*FRT82B/TM6b* (Xu et al., 1995), *w; FRT42D* $hpo^{42\text{-}47}$*CyO* (Wu et al., 2003); *yw hs-FLP; FRT42D Ubi-GFP/CyO*, and *yw hs-FLP; FRT82B Ubi-GFP*. Ectopic expression clones were created by Flip-out with *UAS-Yki* (Huang et al., 2005), *UAS-Yki-S168A*:GFP (Oh and Irvine, 2008), and *yw hs-FLP; act5C > y+ > Gal4 UAS-GFP*.

Taz Genetrap Mice

Taz genetrap embryonic stem cells (BayGenomics; CSD245) were used to generate chimeras by morula aggregation (Wood et al., 1993). Subsequent germline transmission was confirmed by genotyping, reverse transcriptase

(RT)-PCR analysis of embryonic RNA, and immunoblotting for Taz from embryonic lysates (Figure S2).

SUPPLEMENTAL INFORMATION

Supplemental Information includes seven figures and is available with this article online at doi:10.1016/j.devcel.2010.03.007.

ACKNOWLEDGMENTS

We thank Sean Carroll for the anti-Distal-less antibody and Safiah Mohamed Ali for *Taz*$^{-/-}$ kidney sections. This work was supported by grants to L.A. from the Canadian Cancer Society Research Institute and to J.L.W. from the Canadian Institutes of Health Research (Grant #74692). L.A. and J.L.W. hold Canadian Research Chairs, and J.L.W. is an International Scholar of the Howard Hughes Medical Institute. X.V. is supported by a Canadian Cancer Society Research Fellowship.

Received: May 27, 2009
Revised: February 10, 2010
Accepted: March 3, 2010
Published: April 19, 2010

REFERENCES

Aberle, H., Bauer, A., Stappert, J., Kispert, A., and Kemler, R. (1997). β-catenin is a target for the ubiquitin-proteasome pathway. EMBO J. *16*, 3797–3804.

Barrios-Rodiles, M., Brown, K.R., Ozdamar, B., Bose, R., Liu, Z., Donovan, R.S., Shinjo, F., Liu, Y., Dembowy, J., Taylor, I.W., et al. (2005). High-throughput mapping of a dynamic signaling network in mammalian cells. Science *307*, 1621–1625.

Basu, S., Totty, N.F., Irwin, M.S., Sudol, M., and Downward, J. (2003). Akt phosphorylates the Yes-associated protein, YAP, to induce interaction with 14-3-3 and attenuation of p73-mediated apoptosis. Mol. Cell *11*, 11–23.

Bennett, F.C., and Harvey, K.F. (2006). Fat cadherin modulates organ size in *Drosophila* via the Salvador/Warts/Hippo signaling pathway. Curr. Biol. *16*, 2101–2110.

Bryja, V., Schulte, G., and Arenas, E. (2007). Wnt-3a utilizes a novel low dose and rapid pathway that does not require casein kinase 1-mediated phosphorylation of Dvl to activate β-catenin. Cell. Signal. *19*, 610–616.

Chan, E.H., Nousiainen, M., Chalamalasetty, R.B., Schafer, A., Nigg, E.A., and Sillje, H.H. (2005). The Ste20-like kinase Mst2 activates the human large tumor suppressor kinase Lats1. Oncogene *24*, 2076–2086.

Cho, E., Feng, Y., Rauskolb, C., Maitra, S., Fehon, R., and Irvine, K.D. (2006). Delineation of a Fat tumor suppressor pathway. Nat. Genet. *38*, 1142–1150.

Clevers, H. (2006). Wnt/β-catenin signaling in development and disease. Cell *127*, 469–480.

Corbit, K.C., Shyer, A.E., Dowdle, W.E., Gaulden, J., Singla, V., Chen, M.H., Chuang, P.T., and Reiter, J.F. (2008). Kif3a constrains β-catenin-dependent Wnt signalling through dual ciliary and non-ciliary mechanisms. Nat. Cell Biol. *10*, 70–76.

DasGupta, R., Kaykas, A., Moon, R.T., and Perrimon, N. (2005). Functional genomic analysis of the Wnt-wingless signaling pathway. Science *308*, 826–833.

Dong, J., Feldmann, G., Huang, J., Wu, S., Zhang, N., Comerford, S.A., Gayyed, M.F., Anders, R.A., Maitra, A., and Pan, D. (2007). Elucidation of a universal size-control mechanism in *Drosophila* and mammals. Cell *130*, 1120–1133.

Fellouse, F.A., Esaki, K., Birtalan, S., Raptis, D., Cancasci, V.J., Koide, A., Jhurani, P., Vasser, M., Wiesmann, C., Kossiakoff, A.A., et al. (2007). High-throughput generation of synthetic antibodies from highly functional minimalist phage-displayed libraries. J. Mol. Biol. *373*, 924–940.

Hamaratoglu, F., Willecke, M., Kango-Singh, M., Nolo, R., Hyun, E., Tao, C., Jafar-Nejad, H., and Halder, G. (2006). The tumour-suppressor genes NF2/Merlin and Expanded act through Hippo signalling to regulate cell proliferation and apoptosis. Nat. Cell Biol. *8*, 27–36.

Harvey, K.F., Pfleger, C.M., and Hariharan, I.K. (2003). The *Drosophila* Mst ortholog, hippo, restricts growth and cell proliferation and promotes apoptosis. Cell *114*, 457–467.

Hong, J.H., Hwang, E.S., McManus, M.T., Amsterdam, A., Tian, Y., Kalmukova, R., Mueller, E., Benjamin, T., Spiegelman, B.M., Sharp, P.A., et al. (2005). TAZ, a transcriptional modulator of mesenchymal stem cell differentiation. Science *309*, 1074–1078.

Hossain, Z., Ali, S.M., Ko, H.L., Xu, J., Ng, C.P., Guo, K., Qi, Z., Ponniah, S., Hong, W., and Hunziker, W. (2007). Glomerulocystic kidney disease in mice with a targeted inactivation of Wwtr1. Proc. Natl. Acad. Sci. USA *104*, 1631–1636.

Huang, J., Wu, S., Barrera, J., Matthews, K., and Pan, D. (2005). The Hippo signaling pathway coordinately regulates cell proliferation and apoptosis by inactivating Yorkie, the *Drosophila* homolog of YAP. Cell *122*, 421–434.

Kanai, F., Marignani, P.A., Sarbassova, D., Yagi, R., Hall, R.A., Donowitz, M., Hisaminato, A., Fujiwara, T., Ito, Y., Cantley, L.C., et al. (2000). TAZ: a novel transcriptional co-activator regulated by interactions with 14-3-3 and PDZ domain proteins. EMBO J. *19*, 6778–6791.

Labbe, E., Lock, L., Letamendia, A., Gorska, A.E., Gryfe, R., Gallinger, S., Moses, H.L., and Attisano, L. (2007). Transcriptional cooperation between the transforming growth factor-β and Wnt pathways in mammary and intestinal tumorigenesis. Cancer Res. *67*, 75–84.

Lal, M., Song, X., Pluznick, J.L., Di Giovanni, V., Merrick, D.M., Rosenblum, N.D., Chauvet, V., Gottardi, C.J., Pei, Y., and Caplan, M.J. (2008). Polycystin-1 C-terminal tail associates with β-catenin and inhibits canonical Wnt signaling. Hum. Mol. Genet. *17*, 3105–3117.

Lei, Q.Y., Zhang, H., Zhao, B., Zha, Z.Y., Bai, F., Pei, X.H., Zhao, S., Xiong, Y., and Guan, K.L. (2008). TAZ promotes cell proliferation and epithelial-mesenchymal transition and is inhibited by the hippo pathway. Mol. Cell. Biol. *28*, 2426–2436.

London, T.B., Lee, H.J., Shao, Y., and Zheng, J. (2004). Interaction between the internal motif KTXXXI of Idax and mDvl PDZ domain. Biochem. Biophys. Res. Commun. *322*, 326–332.

Makita, R., Uchijima, Y., Nishiyama, K., Amano, T., Chen, Q., Takeuchi, T., Mitani, A., Nagase, T., Yatomi, Y., Aburatani, H., et al. (2008). Multiple renal cysts, urinary concentration defects, and pulmonary emphysematous changes in mice lacking TAZ. Am. J. Physiol. Renal Physiol. *294*, F542–F553.

Mashhoon, N., DeMaggio, A.J., Tereshko, V., Bergmeier, S.C., Egli, M., Hoekstra, M.F., and Kuret, J. (2000). Crystal structure of a conformation-selective casein kinase-1 inhibitor. J. Biol. Chem. *275*, 20052–20060.

McKay, R.M., Peters, J.M., and Graff, J.M. (2001). The casein kinase I family in Wnt signaling. Dev. Biol. *235*, 388–396.

Meignin, C., Alvarez-Garcia, I., Davis, I., and Palacios, I.M. (2007). The salvador-warts-hippo pathway is required for epithelial proliferation and axis specification in *Drosophila*. Curr. Biol. *17*, 1871–1878.

Merkel, C.E., Karner, C.M., and Carroll, T.J. (2007). Molecular regulation of kidney development: is the answer blowing in the Wnt? Pediatr. Nephrol. *22*, 1825–1838.

Miller, B.W., Lau, G., Grouios, C., Mollica, E., Barrios-Rodiles, M., Liu, Y., Datti, A., Morris, Q., Wrana, J.L., and Attisano, L. (2009). Application of an integrated physical and functional screening approach to identify inhibitors of the Wnt pathway. Mol. Syst. Biol. *5*, 315.

Morin-Kensicki, E.M., Boone, B.N., Howell, M., Stonebraker, J.R., Teed, J., Alb, J.G., Magnuson, T.R., O'Neal, W., and Milgram, S.L. (2006). Defects in yolk sac vasculogenesis, chorioallantoic fusion, and embryonic axis elongation in mice with targeted disruption of Yap65. Mol. Cell. Biol. *26*, 77–87.

Nishioka, N., Inoue, K., Adachi, K., Kiyonari, H., Ota, M., Ralston, A., Yabuta, N., Hirahara, S., Stephenson, R.O., Ogonuki, N., et al. (2009). The Hippo signaling pathway components Lats and Yap pattern Tead4 activity to distinguish mouse trophectoderm from inner cell mass. Dev. Cell *16*, 398–410.

Nusse, R. (2005). Wnt signaling in disease and in development. Cell Res. *15*, 28–32.

Oh, H., and Irvine, K.D. (2008). In vivo regulation of Yorkie phosphorylation and localization. Development *135*, 1081–1088.

Park, T.J., Mitchell, B.J., Abitua, P.B., Kintner, C., and Wallingford, J.B. (2008). Dishevelled controls apical docking and planar polarization of basal bodies in ciliated epithelial cells. Nat. Genet. *40*, 871–879.

Riggleman, B., Schedl, P., and Wieschaus, E. (1990). Spatial expression of the *Drosophila* segment polarity gene armadillo is posttranscriptionally regulated by wingless. Cell *63*, 549–560.

Saadi-Kheddouci, S., Berrebi, D., Romagnolo, B., Cluzeaud, F., Peuchmaur, M., Kahn, A., Vandewalle, A., and Perret, C. (2001). Early development of polycystic kidney disease in transgenic mice expressing an activated mutant of the β-catenin gene. Oncogene *20*, 5972–5981.

Saburi, S., Hester, I., Fischer, E., Pontoglio, M., Eremina, V., Gessler, M., Quaggin, S.E., Harrison, R., Mount, R., and McNeill, H. (2008). Loss of Fat4 disrupts PCP signaling and oriented cell division and leads to cystic kidney disease. Nat. Genet. *40*, 1010–1015.

Sansom, O.J., Griffiths, D.F., Reed, K.R., Winton, D.J., and Clarke, A.R. (2005). Apc deficiency predisposes to renal carcinoma in the mouse. Oncogene *24*, 8205–8210.

Saucedo, L.J., and Edgar, B.A. (2007). Filling out the Hippo pathway. Nat. Rev. Mol. Cell Biol. *8*, 613–621.

Silva, E., Tsatskis, Y., Gardano, L., Tapon, N., and McNeill, H. (2006). The tumor-suppressor gene fat controls tissue growth upstream of expanded in the hippo signaling pathway. Curr. Biol. *16*, 2081–2089.

Tian, Y., Kolb, R., Hong, J.H., Carroll, J., Li, D., You, J., Bronson, R., Yaffe, M.B., Zhou, J., and Benjamin, T. (2007). TAZ promotes PC2 degradation through a SCFβ-Trcp E3 ligase complex. Mol. Cell. Biol. *27*, 6383–6395.

Tyler, D.M., and Baker, N.E. (2007). Expanded and fat regulate growth and differentiation in the *Drosophila* eye through multiple signaling pathways. Dev. Biol. *305*, 187–201.

Varelas, X., Sakuma, R., Samavarchi-Tehrani, P., Peerani, R., Rao, B.M., Dembowy, J., Yaffe, M.B., Zandstra, P.W., and Wrana, J.L. (2008). TAZ controls Smad nucleocytoplasmic shuttling and regulates human embryonic stem-cell self-renewal. Nat. Cell Biol. *10*, 837–848.

Wallingford, J.B., and Habas, R. (2005). The developmental biology of Dishevelled: an enigmatic protein governing cell fate and cell polarity. Development *132*, 4421–4436.

Willecke, M., Hamaratoglu, F., Kango-Singh, M., Udan, R., Chen, C.L., Tao, C., Zhang, X., and Halder, G. (2006). The fat cadherin acts through the hippo tumor-suppressor pathway to regulate tissue size. Curr. Biol. *16*, 2090–2100.

Wong, H.C., Bourdelas, A., Krauss, A., Lee, H.J., Shao, Y., Wu, D., Mlodzik, M., Shi, D.L., and Zheng, J. (2003). Direct binding of the PDZ domain of Dishevelled to a conserved internal sequence in the C-terminal region of Frizzled. Mol. Cell *12*, 1251–1260.

Wood, S.A., Pascoe, W.S., Schmidt, C., Kemler, R., Evans, M.J., and Allen, N.D. (1993). Simple and efficient production of embryonic stem cell-embryo chimeras by coculture. Proc. Natl. Acad. Sci. USA *90*, 4582–4585.

Wu, S., Huang, J., Dong, J., and Pan, D. (2003). hippo encodes a Ste-20 family protein kinase that restricts cell proliferation and promotes apoptosis in conjunction with salvador and warts. Cell *114*, 445–456.

Xu, T., and Rubin, G.M. (1993). Analysis of genetic mosaics in developing and adult *Drosophila* tissues. Development *117*, 1223–1237.

Xu, T., Wang, W., Zhang, S., Stewart, R.A., and Yu, W. (1995). Identifying tumor suppressors in genetic mosaics: the *Drosophila* lats gene encodes a putative protein kinase. Development *121*, 1053–1063.

Yu, J., Poulton, J., Huang, Y.C., and Deng, W.M. (2008). The hippo pathway promotes Notch signaling in regulation of cell differentiation, proliferation, and oocyte polarity. PLoS One *3*, e1761.

Zecca, M., Basler, K., and Struhl, G. (1996). Direct and long-range action of a wingless morphogen gradient. Cell *87*, 833–844.

Zhao, B., Lei, Q.Y., and Guan, K.L. (2008). The Hippo-YAP pathway: new connections between regulation of organ size and cancer. Curr. Opin. Cell Biol. *20*, 638–646.